European Journal of Medicinal Chemistry 47 (2012) 452–461

Contents lists available at SciVerse ScienceDirect

European Journal of Medicinal Chemistry

journal homepage: http://www.elsevier.com/locate/ejmech

Original article

Electrochemical and spectroscopic investigations of isoniazide and its analogs with ds.DNA at physiological pH: Evaluation of biological activities

Nasima Arshad [a,*], Uzma Yunus [a], Shumaila Razzque [a], Maliha Khan [a], Samreen Saleem [b], Bushra Mirza [b], Naghmana Rashid [a]

[a] Department of Chemistry, Allama Iqbal Open University, Islamabad, Pakistan
[b] Department of Biochemistry, Quaid-i-Azam University, Islamabad, Pakistan

ARTICLE INFO

Article history:
Received 2 March 2011
Received in revised form
11 October 2011
Accepted 7 November 2011
Available online 18 November 2011

Keywords:
Hydrazids
Cyclic voltammetry
UV–Vis spectroscopy
DNA binding
Binding site size
Biological applications

ABSTRACT

Interaction and binding of isonicotinic acid hydrazide (INH) and its two analogs; pyrazine carboxylic acid hydrazide (PCH) and 2,4-dihydroxy benzoic acid hydrazide (2,4-DHBAH) with DNA has been investigated by UV-spectroscopy and cyclic voltammetry (CV) at physiological conditions of pH and temperature. Experimental results from both techniques were in good agreement and indicated stronger binding and formation of hydrazides–DNA complexes *via* intercalation. Among three hydrazides, 2,4-DHBAH showed greater interaction toward DNA at stomach pH (4.7) as evident from its comparatively greater binding constant, {K_b; 2.02×10^4 M^{-1} (UV), 3.13×10^4 M^{-1} (CV)}. The greater binding site size ($n = 3$) for 2,4-DHBAH at stomach pH inferred 3:1 binding stoichiometry and possibility of electrostatic interactions or hydrogen bonding along with intercalative mode of interaction between 2,4-DHBAH and DNA. The free energies of hydrazides–DNA complexes indicated the spontaneity of their binding. 2,4-DHBAH has shown promising anti-bacterial activities while anti-oxidant and cytotoxic potentials were exhibited by all three hydrazides.

1. Introduction

Interaction between biomolecules is fundamental to numerous biological processes [1]. Based on these interactions living organism maintain complex regulatory and metabolic interactional networks that together constitutes the process of life. A thorough understanding of bimolecular interactions and pathways play key role in solving mystery of life [2].

Many small molecules that bind to DNA are extremely useful as biochemical tools for the visualization of DNA both *in vivo* and *in vitro* and have been clinically proven beneficial although their exact mode of action is unknown [3]. There has been a significant progress made over a past few years in studies of DNA interactions.

Nucleic acids are common targets for antiviral, anticancer and antibiotic drugs [4–6]. A concrete knowledge of drugs nucleic acid interaction, including sequence recognition, structural details, kinetics and thermodynamics of binding is prerequisite for the optimization of drug effectiveness as well as to discover new drugs. The binding interaction of small molecules and their complexes with DNA is of interest for both therapeutic and scientific reasons [7]. These interactions may also be used for conformational recognition to find new structures of DNA and sequence specific differences along the helix of DNA molecule [8–10]. In addition, drug-DNA interaction can be anticipated through electrochemical changes in the redox active molecule of drug [11–14].

Drug can bind to DNA both covalently as well as non-covalently (*via* intercalation mode or minor groove binding). The minor groove of DNA (the negatively charged phosphates outside the DNA double helix) is the locus of action of large numbers of drugs, while in an intercalation mode base pair of DNA unwind to accommodate the drug [15,16]. Both intercalating agents and minor groove binders are typified as anticancer, antiviral and antitumor, anti-bacterial and anti-fungal agents [17–22].

Hydrazides are the effective organic compound having therapeutic properties [23] and known to possess biological effects such as anti-fungal, anti-bacterial and anti-inflammatory activities [24]. A series of substituted hydrazide derivatives have been synthesized and screened for their *in vitro* antimicrobial activities against microorganisms. The results of antimicrobial study indicated that the presence of electron withdrawing groups on the benzoic acid moiety improved antimicrobial activity [25,26]. Isoniazid (INH), rifampin (RIF), ethambutol (EMB) and pyrazinamide (PZA) are well

* Corresponding author. Tel.: +92 51 9057756; fax: +92 51 9250081.
E-mail address: nasimaa2006@yahoo.com (N. Arshad).

0223-5234/$ – see front matter © 2011 Elsevier Masson SAS. All rights reserved.
doi:10.1016/j.ejmech.2011.11.014

known antituberculosis drugs and direct DNA sequencing analysis of their genes *i.e.,* katG, rpoB, embB and pncA, respectively, has been reported as a rapid and useful molecular genetic method for the detection and treatment of drug-resistant *Mycobacterium tuberculosis* [27].

In present studies, an attempt is made to investigate the interaction of isonicotinic acid hydrazide (INH) and its two analogs; pyrazine carboxylic acid hydrazide (PCH) and 2,4-dihydroxy benzoic acid hydrazide (2,4-DHBAH) (Scheme 1) with chicken blood double stranded (ds)-DNA (ck.DNA) using UV–Vis spectroscopic (UV) and cyclic voltammetric (CV) techniques at stomach (4.7) and blood (7.4) pH under body temperature (37 °C). Also these compounds were investigated for anti-bacterial, anti-oxidant and cytotoxic activities.

2. Results and discussion

2.1. DNA binding study by UV-spectroscopy

The binding of drug to DNA has been characterized classically through absorption titrations [28]. Generally, hypochromic (or hyperchromic) effect and red shift (or blue) shift are observed in the absorption spectra of small molecules if they intercalate with DNA [29].

Initially, UV-spectra of pure hydrazides in distilled water were recorded. The UV-spectra of INH, PCH have shown a single intense peak at 263 nm and 270 nm, respectively. 2,4-DHBAH has shown two peaks, one more intense peak at 255 nm while less intense peak at 294 nm. Molar extinction coefficient (ε) of INH, PCH and 2,4-DHBAH were evaluated as; 2632 cm^{-1} M^{-1}, 2873 cm^{-1} M^{-1}, 7546 cm^{-1} M^{-1}, respectively. Since absorption intensity is related to the length of chromophore, longer chromophore showed intense absorption peak. In the case of the three hydrazides the order of absorptions intensity were as follows; 2,4-DHBAH > PCH > INH. Spectrophotometric behavior of INH, PCH and 2,4-DHBAH were studied at two physiological pH (4.7 and 7.4) and at 37 °C using acetate and phosphate buffers, showed no changes in the wavelengths, which may infer non-interactive behavior of hydrazides with buffer solutions.

UV-spectra of three hydrazides were recorded with DNA. Upon addition of various concentrations of DNA on optimized concentrations of INH, PCH and 2,4-DHBAH at both stomach and blood pH and at body temperature, the absorption of the peak intensity increases with a slight blue shift, Figs. 1 & 2. The observed hyperchromic effect upon addition of DNA may correspond to the binding of hydrazide with ds.DNA. As the concentration of DNA is increased more hydrazide bound to DNA and enhanced concentration of hydrazide–DNA complex resulted in hyperchromism. Further, hyperchromic effect may be attributed to either external interaction (electrostatic or groove binding) or to the fact that hydrazide could uncoil DNA double helix [30,31].

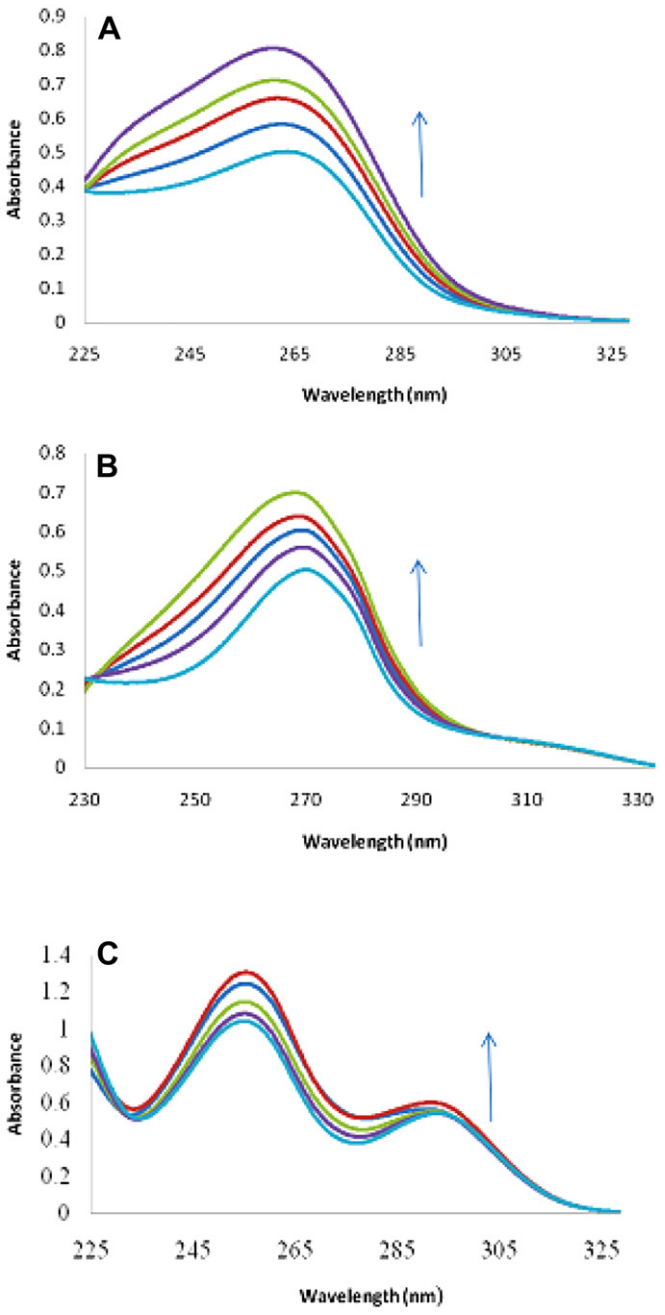

Fig. 1. UV-Spectra for (A) INH, (B) PCH, (C) 2,4-DHBAH (1.1×10^{-4}) without (a) and in the presence of 10 μM (b), 20 μM (c), 30 μM (d), 40 μM (e), and 50 μM (f) DNA at pH 4.7 and at 37 °C. The arrow direction indicates increasing concentrations of DNA.

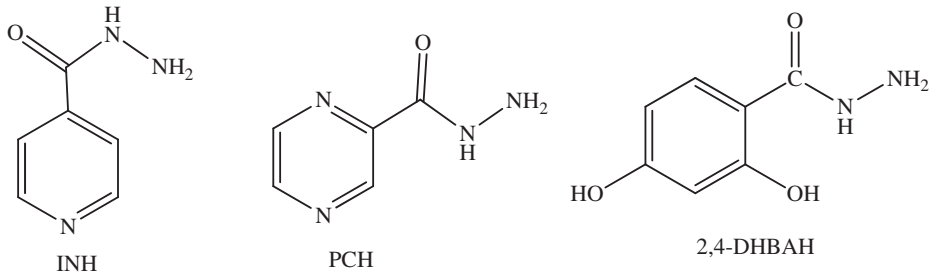

Scheme 1. Structures of hydrazides.

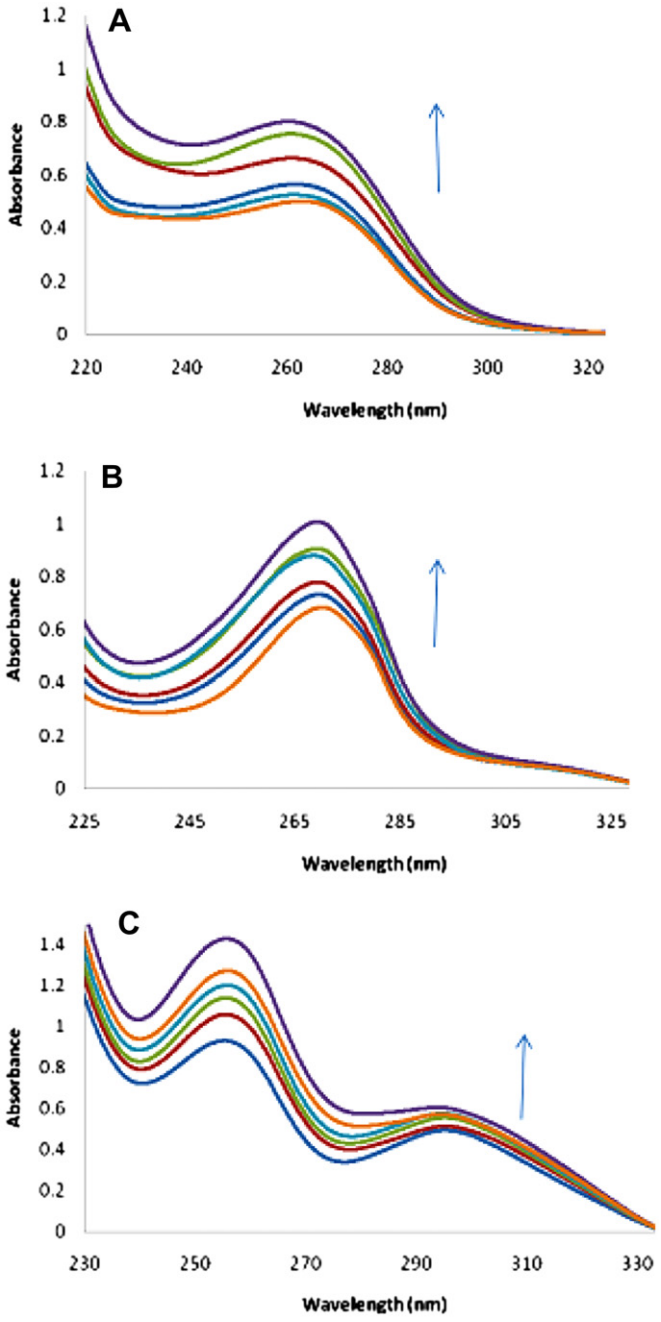

Fig. 2. UV-Spectra for (A) INH, (B) PCH, (C) 2,4-DHBAH (1.1×10^{-4}) without (a) and in the presence of 10 μM (b), 20 μM (c), 30 μM (d), 40 μM (e), and 50 μM (f) DNA at pH 7.4 and at 37 °C. The arrow direction indicates increasing concentrations of DNA.

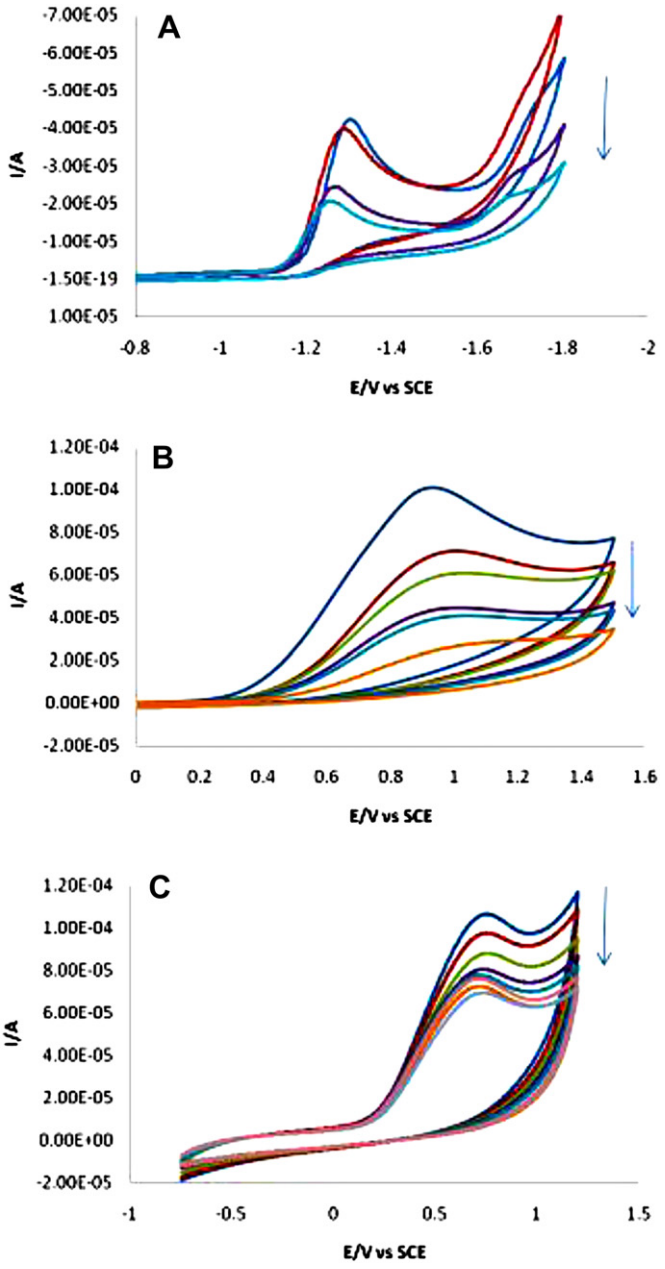

Fig. 3. Cyclic voltammogram for (A) INH, (B) PCH, (C) 2,4-DHBAH (1×10^{-3} M) without (a) and in the presence of 10 μM (b), 20 μM (c), 30 μM (d), 40 μM (e), and 50 μM (f) DNA at pH 4.7 and at 37 °C. The arrow direction indicates increasing concentrations of DNA.

2.2. DNA binding study by cyclic voltammetry

Due to redox activity of most of the small molecules, cyclic voltammetry has proved as one of the important electrochemical technique to elucidate mechanism of drug action *in vivo* [32–34]. The cyclic voltammetric behavior of 1 mM of INH, PCH and 2,4-DHBAH in the absence and presence of 10 μM–50 μM DNA at GCE and under physiological condition of temperature and pH are shown in Figs. 3 & 4. INH showed a single irreversible and stable cathodic (reduction) peak at peak potential of −1.311 V at pH 4.7 and −1.446 V at pH 7.4. PCH and 2,4-DHBAH showed single irreversible anodic peak (oxidation) peaks at +0.9082 V and +0.7393 V, respectively at pH 4.7, and +0.3931 V and +0.5913 V, respectively at pH 7.4, versus SCE.

Upon the addition of various concentrations of DNA on fixed concentration of INH, decrease in the reduction peak current values and a slight positive shift was observed. Cyclic voltammetric behavior of 1 mM of PCH and 2,4-DHBAH in the presence and absence of various concentrations of DNA was also observed as decrease in oxidation peak current and a slight positive shifts in the anodic peak potentials. The substantial diminution in peak current is attributed to the formation of slowly diffusing Hydrazide–DNA supramolecular complex due to which the concentration of the free drug (mainly responsible for the transfer of current) is lowered. A decrease in the peak current along with the positive shifting in the peak potential is attributed to characteristic behavior of the intercalation of drug into DNA double helix [15,35]. Hence the observed behavior of hydrazides in present CV studies for their interaction with ds.DNA could be attributed to the possibility of intercalation

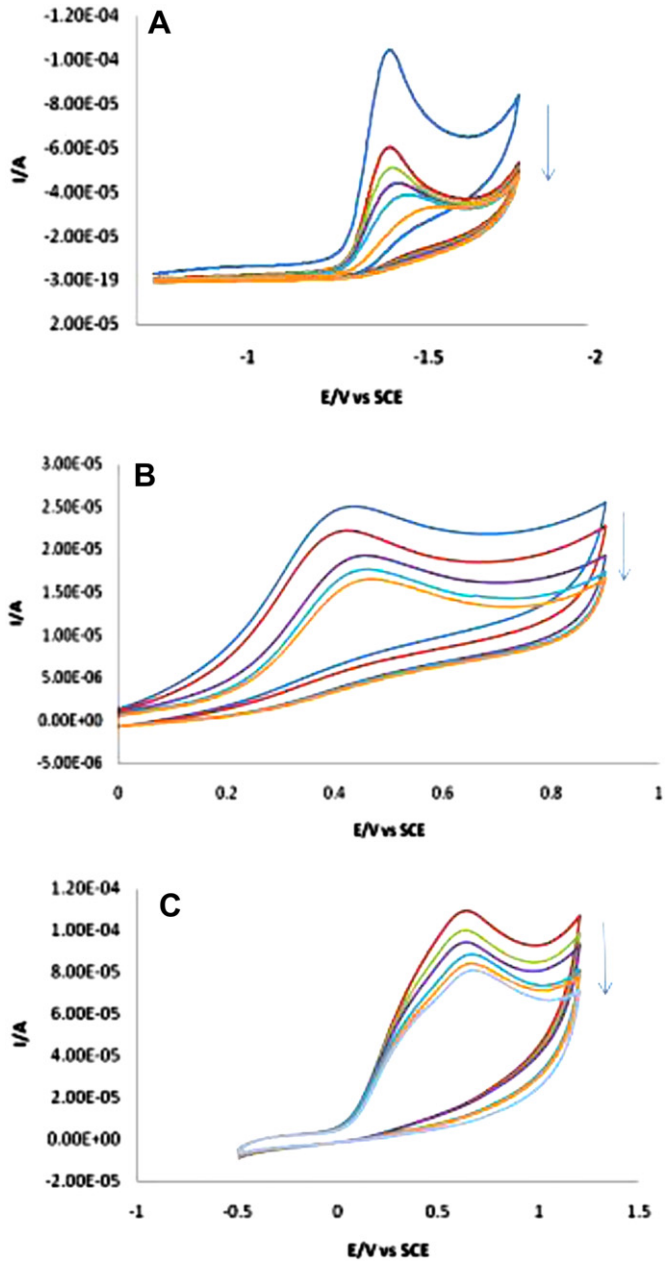

Fig. 4. Cyclic voltammogram for (A) INH, (B) PCH, (C) 2,4-DHBAH (1×10^{-3} M) without (a) and in the presence of 10 μM (b), 20 μM (c), 30 μM (d), 40 μM (e), and 50 μM (f) DNA at pH 7.4 and at 37 °C. The arrow direction indicates increasing concentrations of DNA.

mode. The voltammetric parameters obtained for the three hydrazides with and without DNA are listed in Table 1.

The diffusion coefficients of all the three hydrazides before and after the addition of DNA were measured by using Randles–Sevcik equation [36,37];

$$I_p = 2.99 \times 10^5 n(\alpha n)^{1/2} A C_0^* D^{1/2} \nu^{1/2} \quad (1)$$

Where, I_p is the peak current (A). A is the surface area of the electrode (cm^2), C_0^* is the bulk concentration ($molcm^{-3}$) of the electro active species, D is the diffusion coefficient ($cm^2\ s^{-1}$), α is the transfer coefficient and obtained from $E_p - E_{p/2} = 47.7\ mV/\alpha n$ and ν is the scan rate (Vs^{-1}).

I_p values were plotted *vs.* $\nu^{1/2}$ for hydrazides without and in the presence of DNA, Fig. 5. Cyclic voltammogrames recorded at various scan rates for hydrazides before and after the addition of DNA showed linear dependency of peak currents on the square root of the scan rates. The linearity of the plots verified that the main mass transport of these electro active species (hydrazides) and DNA bound complexes of hydrazides to the electrode surface is diffusion controlled, Fig. 5, [38]. The diffusion coefficients of the free and DNA bound adducts of hydrazides were determined from the slopes of Randles–Sevcik plots. The diffusion coefficient values for INH, PCH and 2,4-DHBAH were calculated $1.79 \times 10^{-7}\ cm^2\ s^{-1}$, $9.89 \times 10^{-9}\ cm^2\ s^{-1}$, $3.17 \times 10^{-7}\ cm^2\ s^{-1}$ without and $4.49 \times 10^{-8}\ cm^2\ s^{-1}$, $7.29 \times 10^{-10}\ cm^2\ s^{-1}$, $1.74 \times 10^{-8}\ cm^2\ s^{-1}$ in the presence of DNA respectively at pH 4.7 and $1.18 \times 10^{-7}\ cm^2\ s^{-1}$, $9.35 \times 10^{-9}\ cm^2\ s^{-1}$, $2.82 \times 10^{-7}\ cm^2\ s^{-1}$ without and $2.56 \times 10^{-9}\ cm^2\ s^{-1}$, $1.09 \times 10^{-9}\ cm^2\ s^{-1}$, $3.21 \times 10^{-9}\ cm^2\ s^{-1}$ in the presence of DNA respectively at pH 7.4. The lower diffusion coefficient values DNA bound hydrazides are responsible for the decay of peak currents in cyclic voltammgrams, Fig. 5.

2.3. Determination of binding constants of hydrazides to DNA by UV-spectrophotometry

Since absorbance is varied after addition of ds.DNA, the binding constant "K_b" of Hydrazides–DNA complex can be determined from the variation in absorbance in UV-spectra. The binding constant values were evaluated for three hydrazides at two physiological pH *i.e.,* 4.7 and 7.4 and at body temperature using Benesi–Hildebrand equation [39–41].

$$\frac{A_0}{A - A_0} = \frac{\varepsilon_G}{\varepsilon_{H-G} - \varepsilon_G} + \frac{\varepsilon_G}{\varepsilon_{H-G} - \varepsilon_G} \frac{1}{K_b[DNA]} \quad (2)$$

Where, K_b is the binding constant. A_0 and A are the absorbance of the free and DNA bound hydrazides complex, ε_G and $\varepsilon_{H\text{-}G}$ are their molar extinction coefficients respectively. From the plot of $A_0/(A-A_0)$ to 1/[DNA], the ratio of the intercept to the slope gave the value of binding constant, K_b, Fig. 6.

K_b values were calculated and given in Table 2. The hydrazide–DNA binding constant values were in range of $10^4\ M^{-1}$ and are in

Table 1
Voltammetric parameters of INH, PCH and 2,4-DHBAH in the presence and absence of DNA at pH 4.7 and 7.4 and at temperature (37 °C).

Complex code	pH 4.7					pH 7.4				
	ν/Vs^{-1}	[DNA]/μM	I/μA	Shift in $E_{p/mV}$	% Decrease in I	ν/Vs^{-1}	[DNA]/μM	I/μA	Shift in $E_{p/mV}$	% Decrease in I
INH	0.1	0	−41.9	51	50.8	0.1	0	−102	8	77.1
INH-DNA	0.1	50	−20.6	–	–	0.1	50	−23.3	–	–
PCH	0.1	0	100	44	75.0	0.1	0	24.3	51	33.3
PCH-DNA	0.1	50	25	–	–	0.1	50	16.3	–	–
2,4-DHBAH	0.1	0	106	20	29.2	0.1	0	108	37	26.1
2,4-DHBAH-DNA	0.1	50	75	–	–	0.1	50	79.8	–	–

% decrease in current $= \frac{(Ip - Ip_0)}{Ip_0} \times 100$

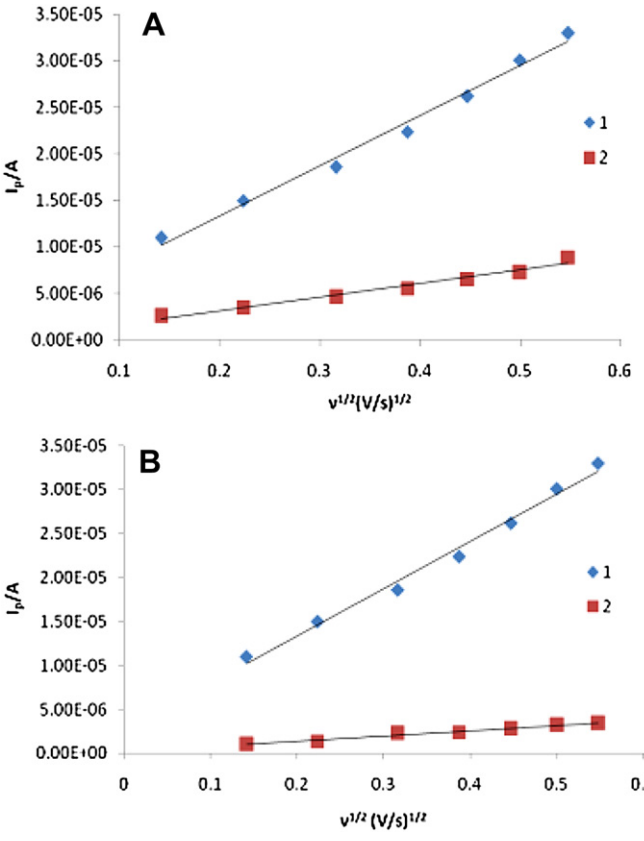

Fig. 5. I_p *vs.* $v^{1/2}$ plots for 1.1×10^{-4} M 2,4-DHBAH at (A) pH 4.7 and (B) 7.4 pH in the absence (1) and in the presence of 50 μL DNA (2) at scan rate of 20 mVs^{-1}, 50 mVs^{-1}, 100 mVs^{-1}, 150 mVs^{-1}, 200 mVs^{-1}, 250 mVs^{-1}, and 300 mVs^{-1} in acetate buffer (pH; 4.7) at 37 °C.

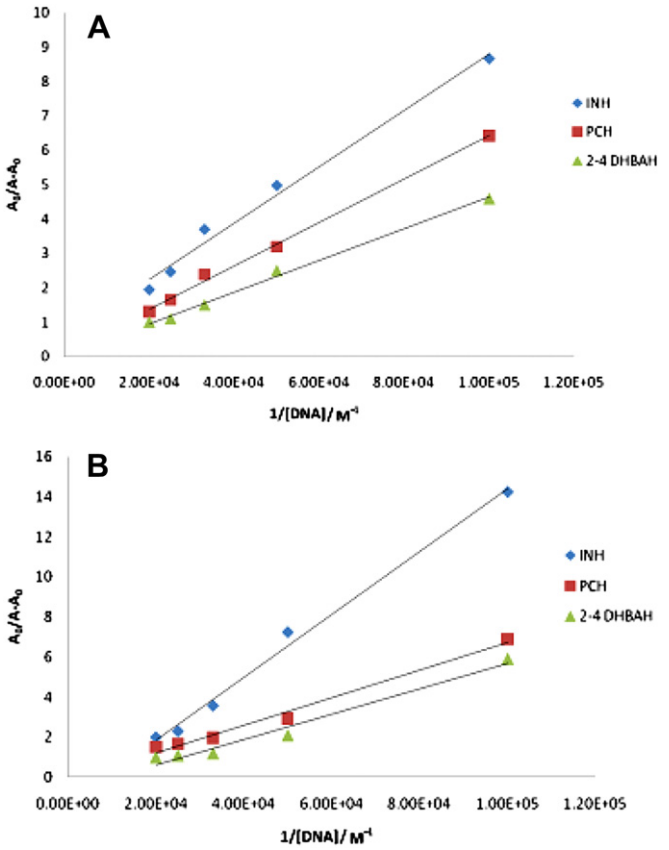

Fig. 6. Plot of $A_0/A\text{-}A_0$ *vs.* 1/[DNA] for the application of Benesi–Hildebrand equation for calculation of hydrazide–DNA binding constant at (A) pH 4.7 and (B) 7.4 pH at 37 °C.

consistent with that reported for the interaction of anthracycline molecules with DNA ($K \approx 10^4 - 10^5\ M^{-1}$). K_b values depicted stronger interactions of the three hydrazides with DNA at both pH values [19,40,42]. UV-spectral changes observed during hydrazide–DNA complex formation *i.e.,* hyperchromic effect and hypsochromic shift in present study inferred the possibility of intercalative mode of interaction. The greater value of binding constant may further be attributed to the small structure of hydrazide molecules whose planer parts may intercalate between the adjacent DNA base pairs.

Binding constant is a measure of the complex stability. In present studies, 2,4-DHBAH showed comparatively greater value of binding constant at stomach pH. The overall data also demonstrated greater binding constant values of the three hydrazides at stomach pH (4.7) as compared to blood pH (7.4), Table 2. The values of binding constants for all the three hydrazides at both pH values are comparable with the binding constant ($1.7 \times 10^4\ M^{-1}$) of a typical intercalator Lumazine. The order of binding constants of three hydrazids was as follows;

$K_{b(2,4\text{-DHBAH})} > K_{b(INH)} = K_{b(PCH)}$ (at stomach pH)
$K_{b(INH)} > K_{b(2,4\text{-DHBAH})} > K_{b(PCH)}$ (at blood pH)

From the values of binding constant "K_b", Gibbs free energies "ΔG" of hydrazides–DNA complexes were calculated, using the following equation;

$$\Delta G = -RT\ln K_b \quad (3)$$

Free energies of all the three hydrazides at both pH values were evaluated as negative values showing the spontaneity of hydrazides–DNA interaction, Table 1 [15,16].

2.4. Evaluation of binding constants and binding sites by cyclic voltammetry

Based upon the decrease in peak current of hydrazides by the addition of different concentration of ds.DNA, the binding constants, K_b for the three hydrazides–DNA complexes were calculated according to the following equation [43].

$$I_p^2 = \frac{1}{K_b[DNA]}\left(I_{p_0}^2 - I_p^2\right) + I_{p_0}^2 - [DNA] \quad (4)$$

Where K_b is the binding constant, I and I_0 are the peak currents with and without DNA. A plot of I_p^2 *vs.* $(I_{p0}^2 - I_p^2)/[DNA]$ gave a straight line with a slope equal to the reciprocal of binding constant, K_b, Fig. 7 (only shown for 2,4-DHBAH–DNA binding). The binding constant values of three hydrazides with DNA were calculated at pH 4.7 and 7.4 and at body temperature (37 °C) and the data are given in Table 3.

The order of binding constants for the three hydrazides obtained by cyclic voltammetric data were as follow;

$K_{b(2,4\text{-DHBAH})} > K_{b(INH)} > K_{b(PCH)}$ (at stomach pH)
$K_{b(INH)} > K_{b(2,4\text{-DHBAH})} > K_{b(PCH)}$ (at blood pH)

The data obtained for K_b from CV were in good agreement as obtained from UV-results and further confirmed the formation of most stable 2,4-DHBAH–DNA complex at stomach pH. From the binding constant data, the standard Gibbs free energy changes for three hydrazides were calculated, Table 2. The negative values of ΔG through voltammetric results also supported the UV-results of free energy changes and indicated the spontaneity of hydrazides–DNA binding.

Table 2
Binding constants and free energy values for the hydrazides–ds.DNA complexes from UV- spectrophotometric data at pH 4.7 and 7.4 and at body temperature (37 °C).

Complex code	pH 4.7		pH 7.4	
	Binding constant K_b/M^{-1}	Free energy (−ΔG) KJmol^{-1}	Binding constant K_b/M^{-1}	Free energy (−ΔG) KJmol^{-1}
INH-DNA	1.60×10^4	24.94	1.42×10^4	24.63
PCH-DNA	1.60×10^4	24.94	1.10×10^4	23.98
2,4-DHBAH-DNA	2.02×10^4	25.54	1.24×10^4	24.29

For the determination of binding site size the following equation was used [44]:

$$C_b/C_f = K[\text{free base pairs}]/s \quad (5)$$

Where, s is the binding site size in terms of base pairs (bp). Measuring the concentration of DNA in terms of hydrazide concentration, the concentration of the base pairs can be expressed as [DNA]/2. So Eq. (5) can be written as:

$$C_b/C_f = K[\text{DNA}]/2s \quad (6)$$

C_f and C_b denote the concentration of the free and DNA bound species respectively. The C_b/C_f ratio was determined by the equation given below [45]:

$$C_b/C_f = I - I_{DNA}/I_{DNA} \quad (7)$$

where I and I_{DNA} represent the peak currents of the hydrazides in the absence and presence of DNA. Putting the value of K_b as calculated according to above Eq. (4), the binding site size of was obtained from the plot of C_b/C_f versus [DNA], Fig. 8 (only shown for 2,4-DHBAH–DNA binding site size).

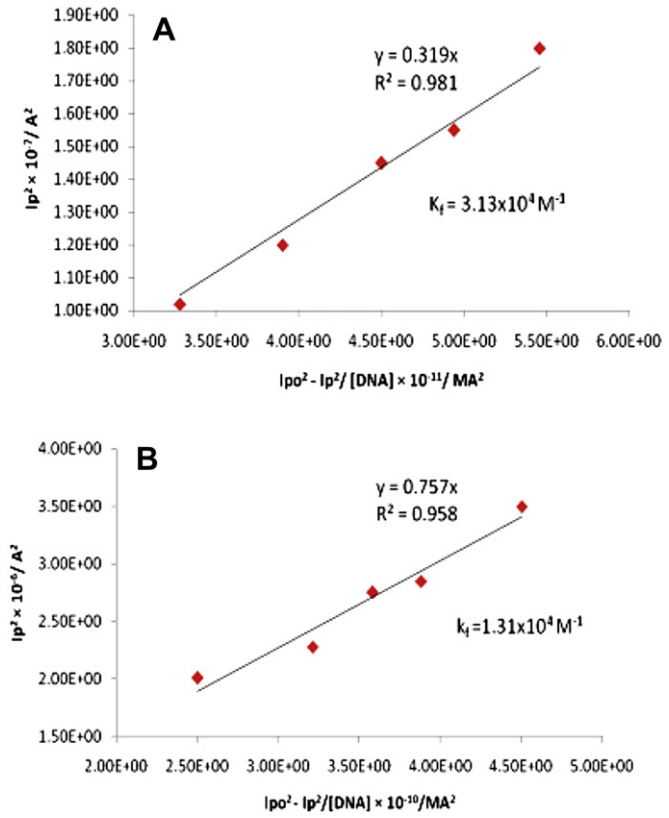

Fig. 7. The plot of I_p^2 *vs.* $I_{po}^2 - I_p^2$/[DNA] for calculation of binding constant of 2,4-DHBAH-DNA adducts at (A) pH 4.7 and (B) 7.4 pH at 37 °C.

Table 3
Binding constants and free energy values for the hydrazides–ds.DNA complexes from voltammetric data at pH 4.7 and 7.4 and at body temperature (37 °C).

Complex Code	pH 4.7		pH 7.4	
	Binding constant K_b/M^{-1}	Free energy (−ΔG) KJmol^{-1}	Binding constant K_b/M^{-1}	Free energy (−ΔG) KJmol^{-1}
INH-DNA	2.03×10^4	25.55	1.60×10^4	24.94
PCH-DNA	1.70×10^4	25.10	1.21×10^4	24.22
2,4-DHBAH-DNA	3.13×10^4	26.67	1.31×10^4	24.45

The binding site size of INH, PCH and 2,4-DHBAH in acetate (pH 4.7) and phosphate (pH 7.4) buffers are calculated as 0.59 bp, 0.23 bp, 3.0 bp and 0.07 bp, 0.03 bp, 1.1 bp, respectively. The binding site size of INH and PCH complexes with DNA implies only a binding site per two base pairs, giving evidences for an intercalation mode, since groove binding and electrostatic binding usually results in significantly higher binding site number [46,47]. However, the greater values of binding site size ($n = 3$) obtained for 2,4-DHBAH at pH 4.7 revealed the existence of electrostatic interactions and hydrogen bonding along with intercalation. The binding site size (n) of 3 for 2,4-DHBAH at stomach pH is comparable with that calculated by Sato et al. [48] and is suggestive of a 3:1 binding stoichiometry of 2,4-DHBAH to the chicken blood ds.DNA.

2.5. Biological studies of hydrazide

2.5.1. Antibacterial activity

The anti-bacterial activity of test compounds (INH, PCH and 2,4-DHBAH) in terms of zone of inhibition (mm) determined through

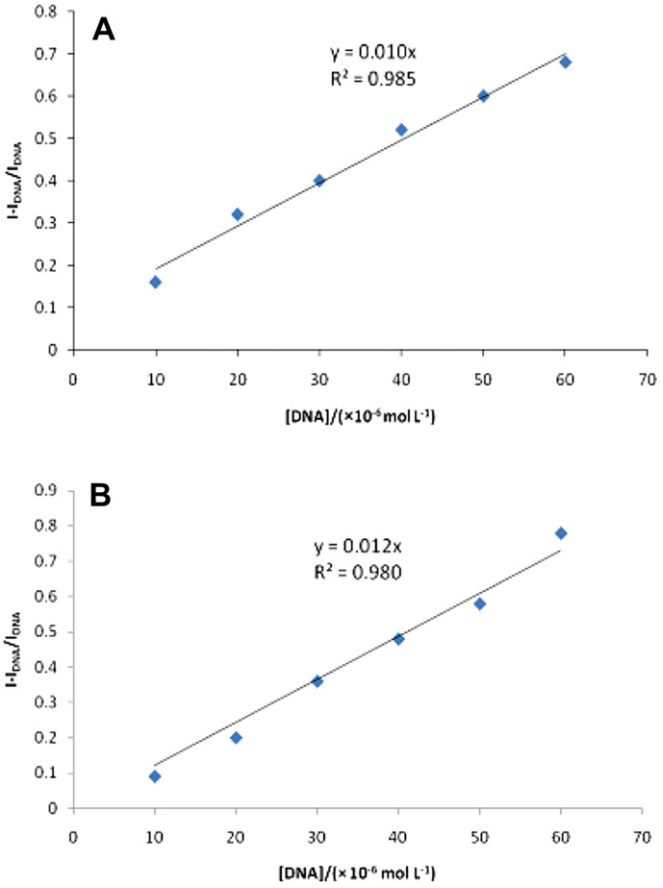

Fig. 8. The plot of C_b/C_f *vs.* [DNA] for determination of binding site size of 2,4-DHBAH-DNA adducts at (A) pH 4.7 and (B) 7.4 pH at 37 °C.

Table 4
Antibacterial activity of hydrazides against different bacterial strains at 1 mg/ml.[a–c]

Compound name	Zones of inhibition (mm)					
	B. bronchiseptica	*E. aerogenes*	*S. typhi*	*E. coli*	*M. luteus*	*S. aureus*
INH	–	–	–	–	–	–
PCH	–	–	–	–	–	–
2,4-DHBAH	18.2	15.3	24.6	25.1	18.2	13.4
Cef[e]	38.5	16.1	34.3	40.5	38.7	39.1
Rox[d]	18.2	31.2	27.9	18.1	30.2	32.0

[a] – = no activity.
[b] Concentrations: 1 $mgml^{-1}$ of DMSO.
[c] Reference drugs.
[d] Roxithromycin 1 $mgml^{-1}$
[e] Cefixime 1 $mgml^{-1}$.

Table 5
MIC of 2,4-DHBAH against different bacterial strains in μg/ml.

Compound name	MIC (μgml^{-1})					
	B. bronchiseptica	*E. aerogenes*	*S. typhi*	*E. coli*	*M. luteus*	*S. aureus*
2,4-DHBAH	800	800	100	100	800	200

agar well diffusion method is shown in Table 4. INH and PCH did not show anti-bacterial activity against any of the bacterial strains used. Even though INH and PCH are particularly used against *M. tuberculosis* but it seems that their activity is highly strain specific. In the present study some other pathogenic bacterial strains were used and the results showed that INH and PCH do not have broad range anti-bacterial activity. However, 2,4-DHBAH, exhibited anti-bacterial activity against all the bacterial strains used. The MIC value of the compound 2,4-DHBAH against six pathogenic bacteria is presented in Table 5.

2.5.2. OH radical induced oxidative DNA damage analysis

INH, PCH and 2,4-DHBAH were investigated *in vitro* at various concentrations (10, 100 and 1000 μgml^{-1}) by using OH radical induced oxidative DNA damage analysis to determine their anti-oxidant and pro-oxidant behavior.

This assay is based on Fenton reaction. Hydrogen peroxide (H_2O_2) is used in this experiment to induce DNA damage by production of free radicals. In Fenton reaction, Fe^{2+} reacts with H_2O_2, resulting in the production of highly reactive hydroxyl radicals, which are considered to be the most harmful radicals to biomolecules. With the attack of OH radicals, if scission occurs on one strand (single stranded nicking) of plasmid DNA, the super-coiled form will be relaxed to generate a slow-moving open-circular form. If both strands of plasmid DNA are cleaved (double stranded nicking), a linear form that migrates between open-circular form and super-coiled form will be generated. Thus, the ability of test compounds to unwind or condense a super-coiling substrate such as plasmid DNA was examined in the present study. This assay is commonly used to check the anti-oxidant or pro-oxidant effects of synthetic as well as natural compounds [49,50].

Evaluation of anti-oxidant or pro-oxidant effects of test compounds on pBR322 plasmid DNA depends on the comparison of intensity of super-coiled monomer in the test with the control. INH was found to be effective DNA-protecting agent at all concentrations tested. PCH protected plasmid DNA at 100 and 1000 μgml^{-1} but it did not reduce the oxidative DNA damage when tested at 10 μgml^{-1} 2,4-DHBAH exhibited protection at lower concentrations (10 and 100 μgml^{-1}) but enhanced the plasmid DNA damage at highest concentration (1000 μgml^{-1}). The reduction in oxidative DNA damage by test compounds indicates amelioration of oxidative stress generation by H_2O_2. These results indicate that all the three compounds could be regarded as potential anti-cancerous agents with further advanced testing and optimization. Results are shown in Fig. 9.

2.5.3. Cytotoxic assay

The cytotoxicity was studied by the brine-shrimp lethality method and the results are summarized in Table 6. Brine shrimp lethality assay is a prescreen assay to test antitumor potential of any compound. The LD_{50} data showed that INH is least cytotoxic (LD_{50} value 1074.75 μgml^{-1}) of all the compounds tested. PCH and 2, 4 DHBAH are cytotoxic with LD_{50} values 312.55 and 418.80 μgml^{-1} respectively.

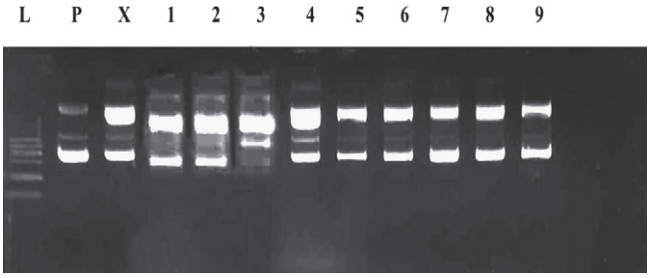

L 1 Kb ladder
P pBR322 plasmid
X pBR322 plasmid treated with $FeSO_4$ and H_2O_2
Lane 1 pBR322 plasmid treated with $FeSO_4$ and H_2O_2 + PCH (1000 μg/ml)
Lane 2 pBR322 plasmid treated with $FeSO_4$ and H_2O_2 + PCH (100 μg/ml)
Lane 3 pBR322 plasmid treated with $FeSO_4$ and H_2O_2 + PCH (10 μg/ml)
Lane 4 pBR322 plasmid treated with $FeSO_4$ and H_2O_2 + 2, 4-DHBAH (1000 μg/ml)
Lane 5 pBR322 plasmid treated with $FeSO_4$ and H_2O_2 + 2, 4-DHBAH (100 μg/ml)
Lane 6 pBR322 plasmid treated with $FeSO_4$ and H_2O_2 + 2, 4-DHBAH (10 μg/ml)
Lane 7 pBR322 plasmid treated with $FeSO_4$ and H_2O_2 + INH (1000 μg/ml)
Lane 8 pBR322 plasmid treated with $FeSO_4$ and H_2O_2 + INH (100 μg/ml)
Lane9 pBR322 plasmid treated with $FeSO_4$ and H_2O_2 + INH (10 μg/ml)

Fig. 9. Effect of PCH, 2,4-DHBAH and INH on pBR322 plasmid DNA.

Table 6
Cytotoxic activity of hydrazides in brine-shrimp lethality assay.

Complex code	LD_{50} value (μgml^{-1})
INH	1074.75
PCH	312.55
2,4-DHBAH	418.80

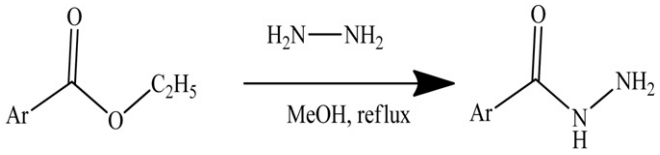

Ar = Pyrazinyl, 2,4-dihydoxyphenyl

Scheme 2. Synthesis of hydrazides (PCH and 2,4-DHBAH).

3. Conclusion

Interactions of three hydrazides; isonicotinic acid hydrazide (INH), pyrazine carboxylic acid hydrazide (PCH) and 2,4-dihydroxy benzoic acid hydrazide (2,4-DHBAH) with chicken blood ds.DNA were investigated through by UV–Vis spectroscopy (UV) and cyclic voltammetry (CV) at stomach (4.7) and blood (7.4) pH under body temperature (37 °C). The results obtained from both techniques revealed intercalation mode of interaction of hydrazides–DNA complexes as the dominant mode. The negative values of standard Gibbs energy changes ($\Delta G = -RTln K_b$) indicated the spontaneity of the binding of three hydrazides with DNA. Other interactional parameters like binding constant and binding site size were determined. The binding constants, K_b, for all the three hydrazides measured by absorbance measurements and changes in voltammetric responses before and after the addition of DNA were in good agreement. The greater interaction of these hydrazides with DNA was evident from their high binding constant values (*i.e.*, in $10^4\ M^{-1}$ orders of magnitude). However, 2,4-DHBAH showed greater affinity to DNA at stomach pH as evident from comparatively greater binding constant values ($2.02 \times 10^4\ M^{-1}$ with UV and $3.13 \times 10^4\ M^{-1}$ with CV studies). The binding site size (n) determined and n value of 3 for 2,4-DHBAH at stomach pH suggested 3:1 binding stoichiometry of 2,4-DHBAH to the chicken blood ds.DNA. Beside the intercalative mode of interaction between 2,4-DHBAH and DNA, electrostatic interactions and hydrogen bonding may also exist due to greater binding site size and presence of OH group in 2,4-DHBAH structure. Linear dependency of peak currents of three hydrazides on the square root of the scan rate before and after the addition of DNA showed that electrochemical processes are diffusion controlled. Among the three hydrazides, 2,4-DHBAH has shown promising broad range anti-bacterial activity while all the three compounds have anti-oxidant and cytotoxic potentials. This study would help to investigate the mechanism of action of hydrazids and to design better and more effective DNA targeted drugs.

4. Experimental

4.1. Reagents and chemicals

INH purchased from Alfa Aesar was further purified by recrystallization using ethanol as a solvent. PCH and 2,4-DHBAH were synthesized from corresponding esters as shown in Scheme 2. Buffer solutions of pH 4.7 (acetate buffer; $CH_3COOH + CH_3COONa$) and pH 7.4 (phosphate buffer; $Na_2HPO_4 + NaH_2PO_4$) were prepared. DNA was extracted in the laboratory from chicken blood by the Falcon method [51] and its concentration was determined spectrophotometrically at 260 nm using molar extinction coefficient, $\varepsilon_{260} = 6600\ cm^{-1}\ M^{-1}$ [52]. Purity of DNA was checked by monitoring the ratio of the absorbance at 260 nm to that at 280 nm and solution gave a ratio of $A_{260}/A_{280} > 1.8$, indicating that DNA was sufficiently pure and free from protein [53]. The stock solutions of INH and its analogs (PCH and 2,4-DHBAH) were prepared by dissolving them in buffer solution of pH 4.7 and 7.4. Autoclaved water was used to prepare all the solutions.

4.2. Instrumentation

The IR spectra of all the three hydrazides were recorded as KBr discs on Bio-Rad Excaliber FT-IR, model FTS 300MX spectrophotometer (USA) in range of 4000–400 cm^{-1}. The electronic absorption spectra were recorded on Shimadzu 1800 spectrophotometer (TCC-240A, Japan) equipped with temperature control device using 1.0 cm matched quartz cells. Cyclic voltammetric experiments were performed using AUTOLAB PGSTAT–302 with GPES version 4.9 (Eco Chemie, Utrecht, Netherlands).

Electrochemical measurements were carried out in a dried conventional three electrode cell using a glassy carbon (GCE; $d = 3$ mm) working electrode, a saturated calomel (SCE; 3.5 M KCl) reference electrode and a Pt sheet counter electrode. Prior to each experiment the GCE was polished with alumina powder and rinsed thoroughly with doubly distilled water for 30 s.

4.3. Synthesis of hydrazides (PCH and 2,4-DHBAH)

The hydrazides (PCH and 2,4-DHBAH) were prepared by refluxing corresponding ester (0.1 mol) with 80% hydrazine hydrate (0.15 mol) in the presence of methanol till the completion of reaction. The mixture was cooled after the completion of reaction and the solid product was collected by filtration and recrystallized from ethanol.

4.3.1. Physical and spectroscopic data of PCH and 2,4-DHBAH

4.3.1.1. Pyrazine carboxylic acid hydrazide (PCH). Reflux time 12 h, orange needle like crystals, m.p.123–125 °C, yield 83.56%.

IR:$\nu(cm^{-1})$ KBr: 3250, 3006, 1701, 1633, 1439.

^{1}H NMR (400 MHz, DMSO-d_6) δppm: 4.62 (s, 2H, NH_2), 8.68 (s, 1H, H5 of pyrazine), 8.81 (d, 1H, $J = 1.60$ Hz, H6 of pyrazine), 9.11 (s, 1H, H_3 of pyrazine), 10.08 (s, 1H, NH).

MS: m/z (%) 138 [M^+](100), 124(5), 105(5).

4.3.1.2. 2,4-Dihydroxy benzoic acid hydrazide (2,4-DHBAH). Reflux time; 10 h, Light brown solid, m.p.194–196 °C, yield 71.43%. IR:$\nu(cm^{-1})$ KBr: 3366, 3302,1634, 1658, 1587.

^{1}H NMR (400 MHz, DMSO): δppm: 9.36 (s,1H), 0.7.32 (s,1H), 6.93 (dd,1H), 6.72 (dd,1H), 4.32 (s,2H), 3.37 (s,1H), 3.29 (s,1H).

MS (EI 70 eV): m/z(%): 168(23), 137(100), 81(55), 69(33), 53(82).

4.4. Procedure for analysis

4.4.1. Spectroscopic titrations

Concentration of DNA determined spectrophotometrically at 260 nm was found 8.4×10^{-5} M. Spectroscopic titrations were carried out at stomach pH (4.7) and blood (7.4) under body temperature (37 °C). The absorbance measurements were performed by keeping the concentration of INH, PCH and 2,4-DHBAH constant (1.1×10^{-4} M) in the sample cell, while varying the concentration of ds.DNA from 10 μM to 50 μM in the sample cell. In order to achieve the equilibrium between the compound and DNA,

solutions were allowed to stay for at least 5 min before each measurements were made. After placing the sample solutions within the cell cavity and before running the spectra, wait for a few seconds till required temperature was attained and shown on temperature controlled device.

4.4.2. Voltammetric assay

First a blank CV was run with the buffer solutions (4.7 and 7.4) at 37 °C, which showed no electroactivity in the potential range of our interest (−2 V to +2 V). Cyclic voltammograms of INH, PCH and 2,4-DHBAH (1 mM) were recorded from −1 V to +1.5 V *vs*. SCE before and after the addition of different volumes (μl) of the stock DNA solution corresponding to the final concentration of DNA ranging from 10 μM to 50 μM within the cell. Scan rate of 100 mVs^{-1} was used throughout the experiments. All measurements were made at 37 °C after purging the solution in the cell with argon gas (99.999%) for at least 10–15 min for flushing out oxygen before every electrochemical assay.

4.4.3. Antibacterial assay

Antimicrobial activity of INH, PCH and 2,4-DHBAH was investigated by using agar well diffusion method [54]. Six bacterial strains; 2 g positive *Staphylococcus aureus* (ATCC 6538), *Micrococcus luteus* (ATCC 10240) and 4 g negative *Enterobacter aerogenes* (ATCC 13048), *Escherichia coli* (ATCC 15224), *Salmonella typhi* (ATCC 6539), *Bordetella bronchiseptica* (ATCC 10580) cultured in LB at 37 °C for 24 h were used. Briefly, the broth culture of each test strain (0.75 ml) was mixed in 75 ml of nutrient agar medium separately and poured into a 14 cm sterile petriplate. After solidification of medium, sterile metallic borer was used to dig 8 mm wells. One hundred micro liters of each test sample (1 $mgml^{-1}$ in DMSO) was poured in its respective well. In each plate DMSO and standard anti-bacterial drugs Roxyithromycin and Cefixime (1 $mgml^{-1}$) served as negative and positive controls respectively. The plates were incubated at 37 °C for 24 h. The anti-bacterial activity was calculated by measuring the diameter of zones of inhibition around each well. The minimum inhibitory concentration (MIC) of active compound was also determined by testing activity of the serial dilutions.

4.4.4. OH radical induced oxidative DNA damage assay

To determine the anti-oxidant (protective) or pro-oxidant (damaging) activity of test compounds (INH, PCH and 2,4-DHBAH), OH radical induced oxidative DNA damage assay was performed [55]. Plasmid pBR322 DNA was diluted using 50 mM phosphate buffer to get a concentration of 0.5 μg/3 μl. Each reaction mixture (15 μl) contained 3 μl of diluted pBR322, 5 μl of test compounds at various concentrations (1000, 100 and 10 μgml^{-1}), 4 μl of 2 mM $FeSO_4$ and 3 μl of 30% H_2O_2. For each experiment, pBR322 DNA treated with 30% H_2O_2 and 2 mM $FeSO_4$ was used as positive control (X). Hydrogen peroxide (H_2O_2) is used because it can induce DNA damage by producing free radicals and $FeSO_4$ acts as a catalyst in this experiment. Untreated pBR322 DNA was used as negative control (P) and a 1 kb DNA ladder (L) was used as marker. Reaction mixtures were incubated at 37 °C for 1 h in dark. All reaction mixtures were subjected to 1% agarose gel electrophoresis in 1X TBE buffer. Ethidium bromide was used to stain DNA bands (super-coiled, linear and open-circular). Gels were visualized under UV, documented (Gel Doc, Bio Rad) and intensity of the bands was determined.

4.4.5. Cytotoxic assay

The cytotoxity was studied by the brine-shrimp lethality assay method [54]. Brine shrimps (*Artemia salina*) were hatched using brine shrimp eggs in sterile artificial sea water (prepared using sea salt 38 gl^{-1}) under constant aeration for 48 h at room temperature. After hatching, active shrimps free from eggs were collected from brighter portion of the hatching chamber and used for the assay. Ten shrimps were drawn through a glass capillary and placed in each vial containing 5 ml of artificial sea water with 10, 100 and 1000 μgml^{-1} final concentration of each test compound from their stock solutions. After 24 h, the number of surviving shrimp was counted (13–15). Experiment was performed in triplicate. Data was analyzed with Finney computer program to determine LD_{50} (Lethal Dose that killed 50% of shrimps) values.

Acknowledgments

The authors are highly grateful to Ms. Asima Siddiqa (National Center for Physics) for technical help in DNA extraction process and Higher Education Commission (HEC) Islamabad Pakistan for financial support.

References

[1] N. Brooijmans, K.A. Sharp, I.D. Kuntz, Proteins 48 (2002) 645–653.
[2] T.L. Blundell, Nature 384 (1996) 23–36.
[3] J.B. Chaires, Curr. Opin. Struct. Biol. 8 (1998) 314–320.
[4] M. Maiti, G.S. Kumar, J. Nucleic Acids 2010 (2010) 23. doi:10.4061/2010/593408 Article ID 593408.
[5] M.J. Waring, Annu. Rev. Biochem. 50 (1981) 159–192.
[6] L.H. Hurley, Biochem. Soc. Trans. 29 (2001) 692–696.
[7] L. Jia, Inorg. Chim. Acta 363 (2010) 855–865.
[8] J.H. Griffin, P.B. Dervan, J. Am.Chem. Soc. 109 (1987) 6840–6842.
[9] J.K. Barton, Science 233 (1986) 727–734.
[10] E. Palecek, M. Fojta, Anal.Chem. 73 (2001) 74A–83A.
[11] S. Takenaka, Y. Uto, H. Kondo, T. Ihara, M. Takagi, Anal. Biochem. 218 (1994) 436–443.
[12] X. Chu, G.L. Shen, J.H. Jiang, T.F. Kang, B. Xiong, R.Q. Yu, Anal. Chem. Acta 373 (1998) 29–38.
[13] M. Aslanoglu, Acta Chem. Slov. 51 (2004) 107–116.
[14] C. Zhoa, J.J. Zhu, J.J. Zhang, H.Y. Chen, Anal. Chem. Acta 394 (1999) 337–344.
[15] M. Aslanoglu, Anal. Sci. 22 (2006) 439–443.
[16] M. Aslanoglu, Turk. J.Chem. 29 (2005) 477–485.
[17] P.G. Baraldi, Med. Res. Rev. 24 (2004) 475–528.
[18] R.R. Monaco, Article ID 702317, J. Nucleic Acids 2010 4, doi:10.4061/2010/702317.
[19] N. Li, L. Ma, C. Yang, L. Guo, X. Yang, Biophys. Chem. 116 (2005) 199–205.
[20] M.S. Shahabuddin, M. Gopal, S.C. Raghavan, J. Cancer Mol. 3 (2007) 139–146.
[21] L.M. Wilhelmsson, N. Kingi, J. Bergman, J. Med. Chem. 51 (2008) 7744–7750.
[22] S. Usha, I.M. Johnson, R. Malathi, Mol. Cell Biochem. 284 (2006) 57–64.
[23] A. Ozdemir, G.T. Zitouni, Z.A. Kaplancikli, Y. Tunali, J. Enzym. Inhib. Med. Chem. 24 (2009) 825–831.
[24] H.M.A. Rahman, M.A. Hussein, Arch. Pharm. (Weinheim) 339 (2006) 378–387.
[25] R.A. Mekheimer, A.M.A. Hameed, K.U. Sadek, ARKIVOC xvi (2008) 144–153.
[26] S. Toliwal, K. Jadav, K. Patel, PMCID, Indian J. Pharm. Sci. 71 (2009) 144–148.
[27] J.H. Choi, Chest 137 (2010) 393–400.
[28] A.M. Pyle, J.P. Rehmann, R. Meshoyrer, C.V. Kumar, N.J. Turro, J.K. Barton, J. Am. Chem. Soc. 111 (1989) 3051–3058.
[29] Y. Sun, S. Bi, D. Song, C. Qiao, D. Mu, H. Zhang, Sensors and Actuators B 129 (2008) 799–810.
[30] A. Tarushi, C.P. Raptopoulou, V. Psycharis, A. Terzis, G. Psomas, D.P. Kessissoglou, Bioorg. Med. Chem. 18 (2010) 2678–2685.
[31] G. Pratviel, J. Bernadou, B. Meunier, Adv. Inorg. Chem. 45 (1998) 251–312.
[32] A. Shah, R. Qureshi, N.K. Janjua, S. Haque, S. Ahmad, Anal. Sci. 24 (2008) 1437–1441.
[33] S. Bollo, L.J.N. Vergara, J.A. Squella, J. Electroanal. Chem. 562 (2004) 9–14.
[34] P.C. Mandal, J. Electroanal. Chem. 570 (2004) 55–61.
[35] X. Lu, M. Zhang, J. Kang, X. Wang, L. Zhuo, H. Liu, J. Inorg. Biochem. 98 (2004) 582–588.
[36] J.E.B. Randles, Trans. Faraday Soc. 44 (1948) 322–327.
[37] A. Sevcik, Collec. Czech. Chem. Commun. 13 (1948) 349–377.
[38] S. Wang, T. Penz, C.F. Yang, Biophys. Chem. 104 (2003) 239–248.
[39] G.J. Yang, J.J. Xu, H.Y. Chen, Z.H. Leng, Chin. J. Chem. 22 (2004) 1325–1329.
[40] M.S. Ibrahim, Anal. Chem. Acta 443 (2001) 63–72.
[41] F. Wang, Y. Xu, J. Zhao, H. Shengshui, J. Bioelectrochem. 70 (2007) 356–362.
[42] H. Berg, G. Horn, U. Luthardt, Bioelectrochem. Bioenergy 8 (1981) 537–553.
[43] J. Niu, G. Cheng, S. Dong, Electrochim. Acta 39 (1994) 2455–2460.
[44] M.T. Carter, M. Rodriguez, A.J. Bard, J. Am. Chem. Soc. 111 (1989) 8901–8911.
[45] M. Aslanoglu, C.J. Isaac, A. Houlton, B.R. Horrocks, Analyst 125 (2000) 1791–1798.
[46] A. Shah, R. Qureshi, A.M. Khan, R.A. Khera, F.L. Ansari, J. Braz. Chem. Soc. 21((2010) 447–451.
[47] Z. Xu, G. Bai, C. Dong, Bioorg. Med. Chem. 13 (2005) 5694–5699.

[48] S. Sato, H. Kondo, T. Nojima, S. Takenaka, Anal.Chem. 77 (2005) 7304–7309.
[49] M. Zaheer, A. Shah, Z. Akhter, R. Qureshi, B. Mirza, M. Tauseef, M. Bolte, Appl. Organomet. Chem. 25 (2011) 61–69.
[50] G. Bibi, I. Haq, N. Ullah, A. Mannan, B. Mirza, Afr. J. Pharm. Pharmacol. 5 (2011) 252–258.
[51] J. Sambrook, E.F. Fritsch, T. Maniatis, Molecular Cloning: A Laboratory Manual Cold Spring Harbor, New York (1989).
[52] M.E. Reichmann, S.A. Rice, C.A. Thomas, P. Doty, J. Am. Chem. Soc. 76 (1954) 3047–3053.
[53] S.S. Babkina, N.A. Ulakhovich, Anal. Chem. 77 (2005) 5678–5685.
[54] M.S. Ahmad, M. Hussain, M. Hanif, S. Ali, M. Qayyum, B. Mirza, Chem. Bio. Drug Des. 71 (2008) 568–576.
[55] H. Nawaz, Z. Akhter, S. Yameen, H.M. Siddiqi, B. Mirza, A. Rifat, J. Organomet. Chem. 694 (2009) 2198–2203.